Proximal methods in tomography CBCT and PET

Jean-François Aujol

IMB, Université Bordeaux 1, UMR CNRS 5251

Joint work with
Sandrine Anthoine, Clothilde Melot (LATP, Marseille)
Yannick Boursier (CPPM, Marseille)

Friday 25th November 2011

Outline

1. CBCT and PET modeling
2. State of the art
3. Recalls in convex analysis
4. CBCT problem : solvers and results on synthetic data
5. PET problem : solvers and results on synthetic data
6. CBCT problem : results on real data
7. Conclusion

Outline

1. CBCT and PET modeling
2. State of the art
3. Recalls in convex analysis
4. CBCT problem : solvers and results on synthetic data
5. PET problem : solvers and results on synthetic data
6. CBCT problem : results on real data
7. Conclusion

CBCT= Cone Beam Computerized Tomography

- CT : a medical imaging modality which provides anatomical information on contrast images.
- CBCT scan : X-ray source+Xray camera, the imaged object in between, in Cone beam geometry.

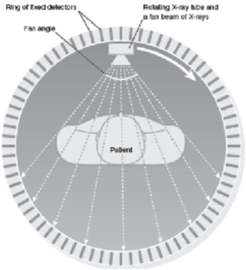

Reminder on CBCT

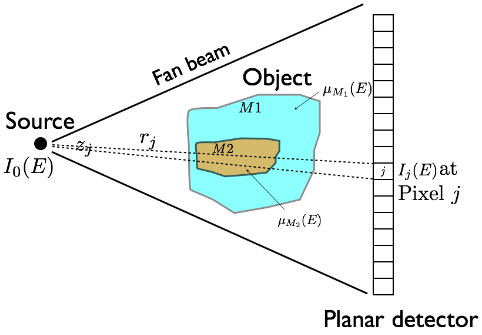

The Beer-Lambert law claims $I_j = z_j \exp\left[-\int_{r_j} \mu_E(l)dl\right]$ with

- $\mu : l \mapsto \mu_E(l)$ the unknown absorption coefficient at point l on r_j.
- z_j a parameter proportional to the number of photons emitted by the source.

Reminder on CBCT, in 3D

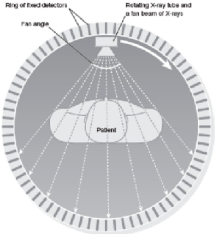

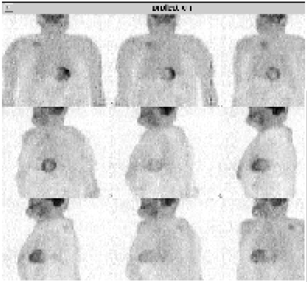

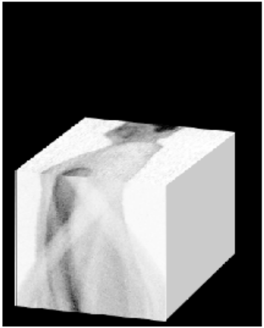

sinogram

Reminder on CBCT, in 3D

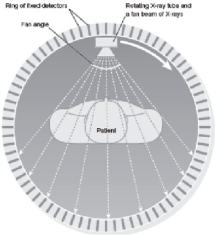

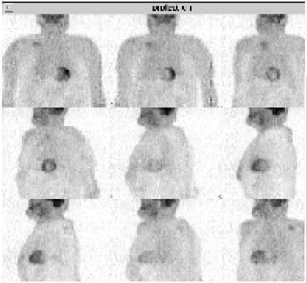

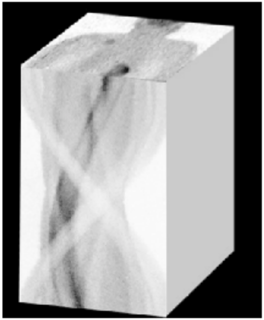

sinogram with more angles

Reminder on PET

PET= Positron Emission Tomography

- PET : medical imaging modality that provides a measurement of the metabolic activity of an organ
- injection to the patient of a radiotracer attached to a molecule that will be absorbed by some organs, depending of their function

$\rightarrow$ radioactive decay emits a positron, which annihilates with an electron after a very short time, and this yields... two gamma rays radiation of 511 keV and opposite direction.
Rings of detectors are supposed to detect them.
parallel-beam geometry

- Possible absorption of photons when crossing the body

- Thus along a line L modeling the measurements :
  $w_L = \int_L x(l) \exp\left(-\mu_{511}(l)\right)$
  - $l \mapsto \mu_{511}(l)$ is supposed to be known.
  - x is the unknown concentration of radioactive desintegration.
- Prototype developped by the CPPM : ClearPET/XPAD (ClearPET developped by EPFL+XPAD developped by CPPM)

$\rightarrow$ allows simultaneous PET/CT imaging based on hybrid pixels

- Hybrid pixels : a new generation of detectors which is in photons counting mode

$\rightarrow$ very low counting rate

- no charge integration : no "dark noise" with these detectors

CBCT framework

no additional gaussian noise in this setting !

- Let $y \in \mathbb{R}^n$ the measurements
- $\mu \in \mathbb{R}^m$ the unknown to recover
- $A \in \mathcal{M}(\mathbb{R}^m, \mathbb{R}^n)$ the system matrix with $n << m$ in general, and ill conditionned.
- pure Poisson noise : $y_j \sim \mathcal{P}\left(z_j \exp\left(-[A\mu]_j\right)\right)$ with $\mathcal{P}(\lambda)$ the Poisson distribution of parameter λ.
- $-\log$ likelihood yields the objective function with constraint $\mu \geq 0$

$$\mathcal{L}_{CBCT}(\mu) = \sum_j y_j[A\mu]_j + z_j \exp\left(-[A\mu]_j\right)$$

- We consider the problem $\hat{\mu} = \arg\min_{\mu \geq 0} \mathcal{L}_{CBCT}(\mu) + \lambda J(\mu)$

PET framework

again no additional gaussian noise in this setting !

- Let $y \in \mathbb{R}^n$ the measurements
- $x \in \mathbb{R}^m$ the unknown to recover
- $B \in \mathcal{M}(\mathbb{R}^m, \mathbb{R}^n)$ the system matrix with $n << m$ in general, and ill conditionned.
- pure Poisson noise : $y_j \sim \mathcal{P}\left([Bx]_j\right)$ with $\mathcal{P}(\lambda)$ the Poisson distribution of parameter λ.
- $-\log$ likelihood yields the objective function with constraint $x \geq 0$

$$\mathcal{L}_{PET}(x) = \sum_j -y_j \log([Bx]_j) + [Bx]_j$$

- We consider the problem $\hat{x} = \arg\min_{x \geq 0} \mathcal{L}_{PET}(x) + \lambda J(\mu)$

Optimization strategy : remarks

- The CBCT data fidelity term is differentiable with our assumption.

$\rightarrow$ Several optimization schemes and penalization can be tested under the constraint that the result $\mu \geq 0$.

- the CBCT optimization problem should be less challenging than the PET one !
- Choice of a regularization term
  - Total-variation $J_{TV}(u) = \sum_{1 \leq i,j \leq N} |(\nabla u)_{i,j}|$
  - Regularized Total-Variation $J_{TV}^{reg} = \sum_{1 \leq i,j \leq N} \sqrt{\alpha^2 + |\nabla u)_{i,j}|^2}$
  - ℓ^1-norm inducing sparsity $J_{\ell^1,\phi}(u) = \sum_{\lambda \in \Lambda} | < u, \phi_\lambda > | = \| R_\phi(u) \|_{\ell^1}$

Outline

1. CBCT and PET modeling
2. State of the art
3. Recalls in convex analysis
4. CBCT problem : solvers and results on synthetic data
5. PET problem : solvers and results on synthetic data
6. CBCT problem : results on real data
7. Conclusion

Quick non exhaustive review

- some algorithms to recover CBCT and PET images viewed as Poisson noisy data
  - Filtered backprojection for Cone Beam geometry : FDK algorithm (Feldkamp and all 1984...)
  - EM algorithm and variants (Shepp and Vardi 1982, Lange and Carson 1984, Hudson and Larkin 1994...)
  - Regularization of EM type algorithms : quadratic surrogate functions (De Pierro 1994, Fessler and all 1998...), Huber (Chlewicki and all 2004...), TV (Harmany and all 2011...)

$\rightarrow$ technics closed to the ones used in convex optimization

Quick non exhaustive review

- Forward backward splitting (Combettes-Wajs 2005) after using an Anscombe transform to go back to Gaussian noise applied in the setting of Deconvolution problems with Poisson noisy data (Dupé et al 2009)
- Alternative Direction Method of Multipliers in the context of poissonian image reconstruction (Figueiredo 2010)
- PPXA algorithm applied in the context of dynamical PET (Pustelnik et al 2010)
- Primal dual algorithm using TV regularization in the context of blurred Poisson noisy data (Bonettini and Ruggiero 2010)
- Remember Gabriel Peyré's talk this morning
- ...

Outline

1. CBCT and PET modeling
2. State of the art
3. Recalls in convex analysis
4. CBCT problem : solvers and results on synthetic data
5. PET problem : solvers and results on synthetic data
6. CBCT problem : results on real data
7. Conclusion

Proximal operator

Let F be a convex proper function. We recall that the subgradient of F, which is denoted by ∂F, is defined by

$$\partial F(x) = \{p \in X \text{ such that } F(y) \geq F(x) + \langle p, y - x \rangle \ \forall y\}$$

For any $h > 0$ the following problem always has a unique solution :

$$\min_y hF(y) + \frac{1}{2}\|x - y\|^2$$

This solution is given by :

$$y = (I + h\partial F)^{-1}(x) = \mathrm{prox}_h^F(x)$$

The mapping $(I + h\partial F)^{-1}$ is called the *proximity* operator.

Examples

$$\min_y hF(y) + \frac{1}{2}\|x - y\|^2$$

- When F is the indicator function of some closed convex set C, i.e. :
$$F(x) = \begin{cases} 0 \text{ if } x \in C \\ +\infty \text{ otherwise} \end{cases}$$
then $\mathrm{prox}_h^F(x)$ is the orthogonal projection of x onto C.
- When $F(x) = \|x\|_{\dot{B}^1_{1,1}}$, then $\mathrm{prox}_h^F(x)$ is the soft wavelet shrinkage of x with parameter h.
- When $F(x) = J_{TV}(x)$ then $\mathrm{prox}_h^F(x) = x - hP_{hK}(x)$, with P_{hK} orthogonal projection onto hK, and $K = \{\mathrm{div}\, g \ / \ |g_{i,j}| \leq 1 \ \forall i,j\}$.

Forward-backward splitting

$$\min_x F(x) + G(x)$$

where F is a convex $C^{1,1}$ function, with ∇F L Lipschitz, and G a simple convex function (simple means that the *proximity* operator of G is easy to compute).
The Forward-Backward algorithm reads in this case :

$$\begin{cases} x_0 \in X \\ x_{k+1} = \quad (I + h\partial G)^{-1}(x_k - h\nabla F(x_k)) = \mathrm{prox}_h^G(x_k - h\nabla F(x_k)) \end{cases}$$

This algorithm is known to converge provided $h \leq 1/L$. In terms of objective functions, the convergence speed is of order $1/k$.

It has been shown by Nesterov (2005) and by Beck-Teboule (2009) that the previous algorithm could be modified so that a convergence speed of order $1/k^2$ is obtained.
The FISTA algorithm proposed by Beck and Teboule is the following :

$$\begin{cases} x_0 \in X & ;\ y_1 = x_0;\ t_1 = 1; \\ x_k = & (I + h\partial G)^{-1}(y_k - h\nabla F(y_k)) \\ t_{k+1} = & \frac{1+\sqrt{1+4t_k^2}}{2} \\ y_{k+1} = & x_k + \frac{t_k - 1}{t_{k+1}}(x_k - x_{k-1}) \end{cases}$$

This algorithm converges provided $h \leq 1/L$.

Beck and Teboule have shown that FISTA could be used to solve the constrained total variation problem.

$$\min_{u \in C} J_{TV}(u) + \frac{1}{2\lambda}\|f-u\|^2 \qquad (1)$$

with C a closed non empty convex set.

Proposition : Let us set :

$$h(v) = -\|H_C(f-\lambda \operatorname{div} v)\|^2 + \|f-\lambda \operatorname{div} v\|^2$$

where $H_C(u) = u - P_C(u)$ and $P_C(u)$ is the orthogonal projection of u onto C. Let us define :

$$\tilde{v} = \arg\min_{\|v\|\leq 1} h(v)$$

Then the solution of problem (1) is given by :

$$u = P_C(f - \lambda \operatorname{div} \tilde{v})$$

FISTA and constrained regularization

The previous result can be adapted to some general L^1 regularization :

$$\min_{u \in C} \|Ku\|_1 + \frac{1}{2\lambda}\|f - u\|^2 \quad (1)$$

with C a closed non empty convex set. K is a continuous linear operator from X to Y (two finite-dimensional real vector spaces).
Proposition : Let us set :

$$h_K(v) = -\|H_C(f + \lambda K^* v)\|^2 + \|f + \lambda K^* v\|^2$$

where $H_C(u) = u - P_C(u)$ and $P_C(u)$ is the orthogonal projection of u onto C. Let us define :

$$\tilde{v} = \arg\min_{\|v\| \leq 1} h_K(v)$$

Then the solution of problem (1) is given by :

$$u = P_C(f + \lambda K^* \tilde{v})$$

Chambolle-Pock algorithm

X and Y are two finite-dimensional real vector spaces. $K : X \to Y$ continuous linear operator. F and G convex functions.

$$\min_{x \in X} \left(F(Kx) + G(x) \right)$$

We remind the definition of the Legendre-Fenchel conjugate of F :

$$F^*(y) = \max_{x \in X} \left(\langle x, y \rangle - F(x) \right) \tag{1}$$

The associated saddle point problem is :

$$\min_{x \in X} \max_{y \in Y} \left(\langle Kx, y \rangle + G(x) - F^*(y) \right)$$

$\Longrightarrow$ Arrow-Urwicz method (ascent in y, descent in$x$).

Chambolle-Pock algorithm

$$\min_{x \in X} \max_{y \in Y} \left(\langle Kx, y \rangle + G(x) - F^*(y) \right) \tag{1}$$

- *Initialization :* Choose $\tau, \sigma > 0$, $(x_0, y_0) \in X \times Y)$, and set $\bar{x}_0 = x_0$.
- *Iterations ($n \geq 0$) :* Update $x_n, y_n, \bar{x}_n$ as follows :

$$\begin{cases} y_{n+1} = (I + \sigma \partial F^*)^{-1}(y_n + \sigma K \bar{x}_n) \\ x_{n+1} = (I + \tau \partial G)^{-1}(x_n - \tau K^* y_{n+1}) \\ \bar{x}_{n+1} = 2x_{n+1} - x_n \end{cases} \tag{2}$$

Theorem

Let $L = \|K\|$, and assume problem (1) has a saddle point. Choose $\tau \sigma L^2 < 1$, and let $(x_n, \bar{x}_n, y_n)$ be defined by (2). Then there exists a saddle point (x^*, y^*) such that $x^n \to x^*$ and $y^n \to y^*$.

Notice that both F and G can be non smooth.

Outline

1. CBCT and PET modeling
2. State of the art
3. Recalls in convex analysis
4. CBCT problem : solvers and results on synthetic data
5. PET problem : solvers and results on synthetic data
6. CBCT problem : results on real data
7. Conclusion

Solving the CBCT problem

$$\sum_j y_j [A\mu]_j + z_j \exp\left(-[A\mu]_j\right) + \chi_{\{\mu \geq 0\}} + \lambda J(\mu)$$

belongs to the class of problems $\arg\min_{x \in X} F(x) + G(x)$

- with F and G proper, convex, lower semi-continuous functions, and F L Lipschitz differentiable
- recall the definition $prox_F(x) = \arg\min_{y \in X} F(y) + \frac{1}{2} \parallel x - y \parallel^2$
- **Forward-backward splitting iterations** (Combettes-Wajs 2005, Daubechies-De Mol 2004)
  $x_{k+1} = prox_{hG}(x_k - h\nabla F(x_k))$. Converge if $h \leq \frac{1}{L}$.
- with $G = \lambda J_{TV} + \chi_C$ ($C = \{x \geq 0\}$) can be solved with the algorithm **FISTA** (Beck and Teboulle 2009)
- with $G = \lambda J_{\ell^1,\phi} + \chi_C$, can be solved using again **FISTA**

Algorithms for CBCT

- **[TVreg]** using J_{TV}^{reg}, accelerated projected gradient descent.
- **[FB-TV]** using J_{TV}, Forward-Backward algorithm combined with FISTA.
- **[FB-wav]** using $J_{\ell^1,\phi}$, Forward-Backward algorithm combined with FISTA.

$\rightarrow$ tested against three algorithms implemented in the IRT toolbox

- **[FBP]** Filtered backprojection
- **[MLEM]** MLEM algorithm
- **[MLEM-H]** MLEM algorithm penalized by a Huber function.

→ Simulated phantoms to recover :


Zubal

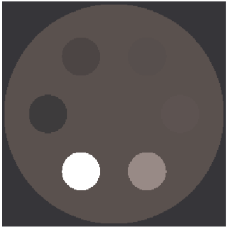
Contrast

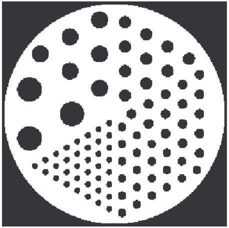
Resolution

→ Criteria, T being the true object and I the reconstructed image

$$SNR(I,T) = 10\log_{10}\left(\frac{\mathrm{mean}(I^2)}{\mathrm{mean}(|I-T|^2)}\right)$$

$$SSIM(I,T) = \mathrm{mean}_w\left(\frac{(2\,\mathrm{mean}(I_w)\mathrm{mean}(T_w)+a)(2\,\mathrm{cov}(I_w,T_w)+b)}{\mathrm{mean}(I_w)^2+\mathrm{mean}(T_w^2+a)(\mathrm{var}(I_w)+\mathrm{var}(T_w)+b)}\right)$$

$$CNR(I) = \frac{|\mathrm{mean}(I_{in})-\mathrm{mean}(I_{out})|}{\sqrt{\mathrm{var}(I_{in})+\mathrm{var}(I_{out})}}$$

CBCT Zubal $z = 1e3$ photons

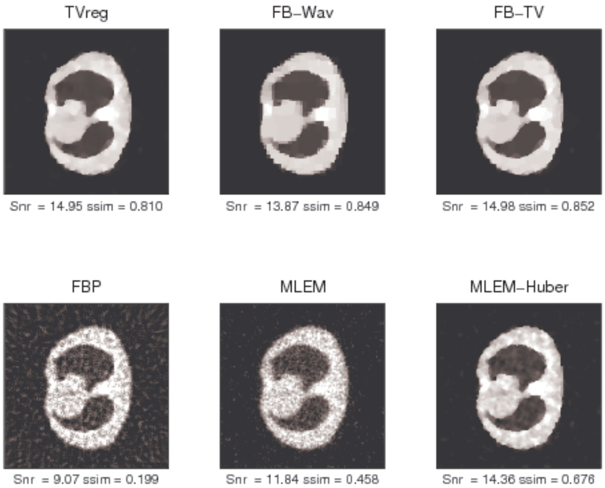

CBCT Zubal $z = 1e2$ photons

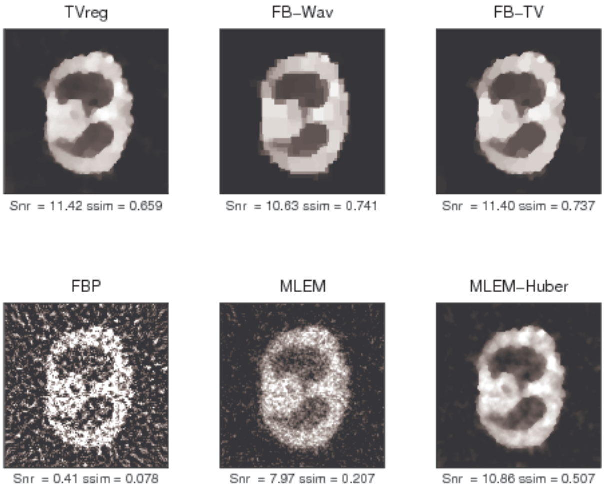

CBCT $z = 1e3$ and $z = 1e2$

Photon count	Algorithm	SNR	SSIM	λ	nb. iter.	time (s)
1e3	TVreg	15.06	0.808	200	300	36
	FB-Wav	14.06	0.826	25	300	110
	FB-TV	15.10	0.845	200	300	85
	FBP	9.08	0.201	-	-	0.09
	MLEM	11.86	0.462	-	43	14
	MLEM-H	14.52	0.680	7e5	752	
1e2	TVreg	11.34	0.625	80	300	32
	FB-Wav	10.62	0.695	10	300	110
	FB-TV	11.35	0.690	80	300	78
	FBP	0.44	0.076	-	-	0.07
	MLEM	7.90	0.200	-	17	5.67
	MLEM-H	10.78	0.489	3.5e4	605	

CBCT Contrast for 60 projections

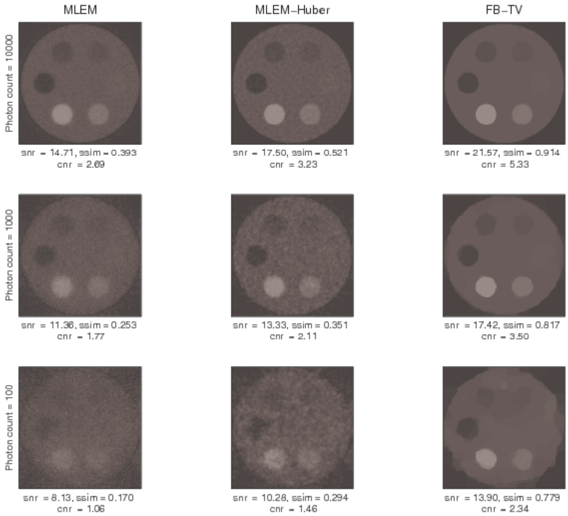

CBCT Contrast for 60 projections

photon count	Algorithm	CNR	SSIM	SNR
1e4	FB-Wav	4.18	0.911	20.09
	FB-TV	5.33	0.914	21.57
	MLEM-H	3.23	0.521	17.50
1e3	FB-Wav	2.96	0.839	17.01
	FB-TV	3.50	0.817	17.42
	MLEM-H	2.11	0.351	13.33
1e2	FB-Wav	2.08	0.779	12.93
	FB-TV	2.34	0.779	13.90
	MLEM-H	1.46	0.294	10.28

Influence of the number of projections

	Nb. angles	90			60		
Photon count	Algorithm	CNR	SSIM	SNR	CNR	SSIM	SNR
1e3	TVreg	3.17	0.793	17.15	3.00	0.743	16.95
	FB-Wav	3.18	**0.851**	**17.68**	2.96	**0.839**	17.01
	FB-TV	**3.93**	0.831	17.65	**3.50**	0.817	**17.42**
	FBP	0.82	0.046	3.57	0.65	0.033	2.09
	MLEM	1.95	0.274	11.87	1.77	0.253	11.36
	MLEM-H	2.27	0.337	13.49	2.11	0.351	13.33

	Nb. angles	30		
1e3	TVreg	2.78	0.728	**15.46**
	FB-Wav	2.61	**0.802**	15.39
	FB-TV	**3.36**	0.756	15.25
	FBP	0.44	0.017	-0.79
	MLEM	1.53	0.218	10.33
	MLEM-H	2.04	0.393	13.47

CBCT Resolution for 60 projections

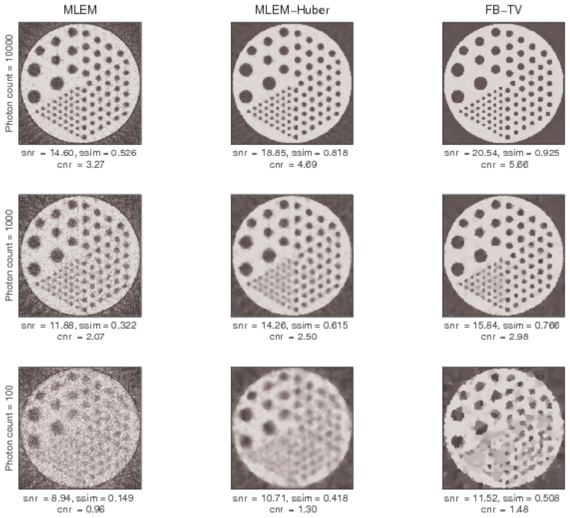

Outline

1. CBCT and PET modeling
2. State of the art
3. Recalls in convex analysis
4. CBCT problem : solvers and results on synthetic data
5. PET problem : solvers and results on synthetic data
6. CBCT problem : results on real data
7. Conclusion

Solving the PET problem

$$\sum_j -y_j \log([Bx]_j) + [Bx]_j + \chi_{\{x \geq 0\}} + \lambda J(x)$$

belongs to the class of problems $\arg\min_{x \in X} F(Kx) + G(x)$

- with F and G proper, convex, lower semi-continuous functions, F and G non differentiable, K a continuous linear operator
- Primal-dual algorithm : **Chambolle-Pock algorithm** (2010)

$$\left\{ \begin{array}{l} y_{n+1} = prox_{\sigma F^\star}(y_n + \sigma K \bar{x}_n) \\ x_{n+1} = prox_{\tau G}(x_n - \tau K^* y_{n+1}) \\ \bar{x}_{n+1} = 2x_{n+1} - x_n \end{array} \right.$$

Application of CP scheme

$C = \{x \geq 0\}$

- 1rst version : $\min_x F(Bx) + G(x)$
  - $F(x) = \sum_j x_j - w_j \log(x_j) + \chi_C(x)$
  - $G(x) = \lambda J(x) + \chi_C(x)$.
- 2nd version : $\min_x F(Bx) + G(Kx) + \chi_C(x)$
  - $F(x) = \sum_j x_j - w_j \log(x_j) + \chi_C(x)$
  - $G(p) = \| p \|_1$ and $K = \nabla$ or $K = R_\phi$.
  - Associated saddle point problem :

$$\min_x \max_{y,z} \left(\langle Kx, y \rangle + \langle Bx, z \rangle - F^*(y) - G^*(z) + \chi_C(x) \right)$$

Algorithms for PET

- Regularized version of the data fidelity term
  $\mathcal{L}^{\varepsilon}_{PET}(x) = \sum_j -y_j \log([Bx]_j + \varepsilon) + [Bx]_j$

$\rightarrow$ Forward Backward type algorithms can used.

- **[CP-TV-BT]** using J_{TV}, first approach of Chambolle-Pock combined with FISTA
- **[CP-TV]** using J_{TV}, second approach of Chambolle-Pock
- **[CP-wav]** $J_{\ell^1,\phi}$, Chambolle-Pock algorithm

$\rightarrow$ tested against the same three algorithms implemented in the IRT toolbox

- **[FBP]** Filtered backprojection, **[MLEM]** MLEM algorithm, **[MLEM-H]** MLEM algorithm penalized by a Huber function.
- and **[SPIRAL]** an algorithm very closed to Forward Backward algorithm

Results on simulated data

$\rightarrow$ Simulated phantoms to recover :

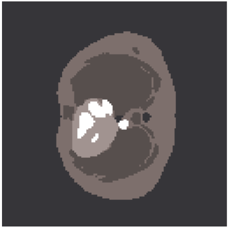

Zubal

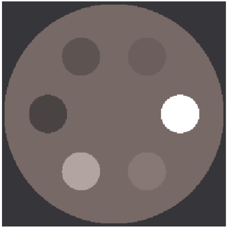

Contrast

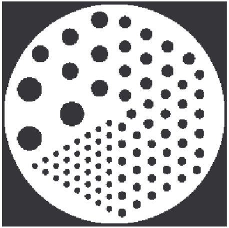

Resolution

$\rightarrow$ Recall the criteria, with T the original image

$$SNR(I,T) = 10\log_{10}\left(\frac{\mathrm{mean}(I^2)}{\mathrm{mean}(|I-T|^2)}\right)$$

$$SSIM(I,T) = \mathrm{mean}_w\left(\frac{(2\mathrm{mean}(I_w)\mathrm{mean}(T_w)+a)(2\,\mathrm{cov}(I_w,T_w)+b)}{\mathrm{mean}(I_w)^2+\mathrm{mean}(T_w^2+a)(\mathrm{var}(I_w)+\mathrm{var}(T_w)+b)}\right)$$

$$CNR(I) = \frac{|\mathrm{mean}(I_{in})-\mathrm{mean}(I_{out})|}{\sqrt{\mathrm{var}(I_{in})+\mathrm{var}(I_{out})}}$$

PET , fcount = 500 000

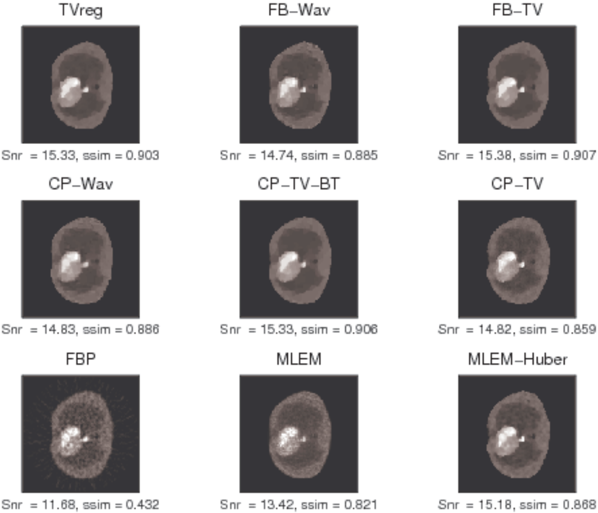

PET , fcount = 500 000

Algorithm	SNR	SSIM	λ	nb. iter.	time (s)
TVreg	15.33	0.902	0.70	200	10
FB-Wav	14.77	0.889	0.10	150	89
FB-TV	15.37	0.905	0.70	100	62
CP-Wav	14.68	0.885	0.10	80	63
CP-TV-BT	15.32	0.905	0.70	80	63
CP-TV	14.84	0.860	0.70	400	266
SPIRAL	15.17	0.905	0.70	100	76
FBP	11.59	0.429	-	-	0.04
MLEM	13.38	0.819	-	17	2
MLEM-H	15.22	0.866	0.9/0.25	267	46

PET , fcount = 100 000

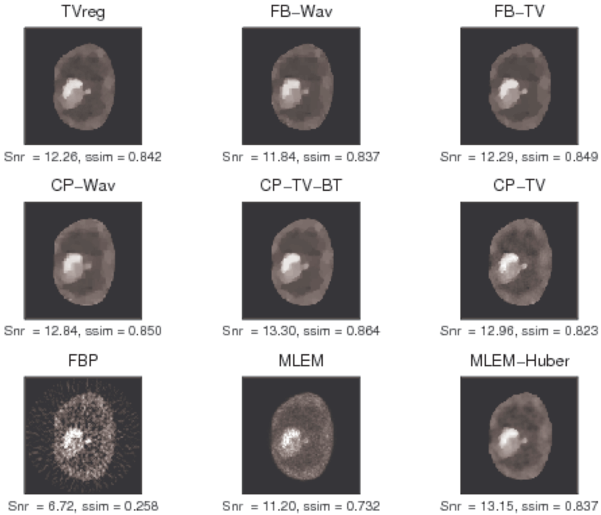

Algorithm	snr	ssim	λ	nb. iterations	time (s)
TVreg	12.12	0.841	0.40	200	13
FBwav	11.55	0.834	0.0625	150	89
FB-TV	12.14	0.847	0.40	100	68
CPwav	11.65	0.835	0.0625	50	40
CP-TV-BT	13.13	0.862	0.40	50	46
CP-TV	12.86	0.823	0.40	100	78
SPIRAL	11.77	0.841	0.40	100	86
FBP	6.66	0.254	-	-	0.08
MLEM	11.06	0.731	-	10	2
MLEM-H	12.92	0.837	0.8/0.25	278	58

PET Contrast for $fcount = 2e5$

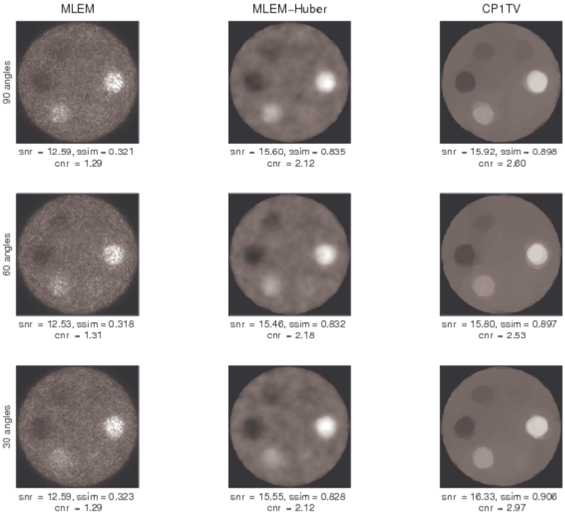

PET Contrast

for $fcount = 2e5$

N. angles	30			60			90		
Algo	CNR	SSIM	SNR	CNR	SSIM	SNR	CNR	SSIM	SNR
CP-TV-BT	2.60	0.898	15.92	2.53	0.897	15.80	2.97	0.906	16.33
MLEM	1.29	0.321	12.59	1.31	0.318	12.53	1.29	0.323	12.59
MLEM-H	2.12	0.835	15.60	2.18	0.832	15.46	2.12	0.828	15.55

for $fcount = 1e5$

N. angles	30			60			90		
Algo	CNR	SSIM	SNR	CNR	SSIM	SNR	CNR	SSIM	SNR
CP-TV-BT	2.64	0.900	16.11	2.55	0.897	15.84	2.72	0.901	15.92
MLEM	1.62	0.405	14.00	1.59	0.418	13.91	1.67	0.428	14.14
MLEM-H	2.67	0.842	17.50	2.42	0.837	17.24	2.59	0.842	17.39

PET Resolution for $fcount = 2e5$

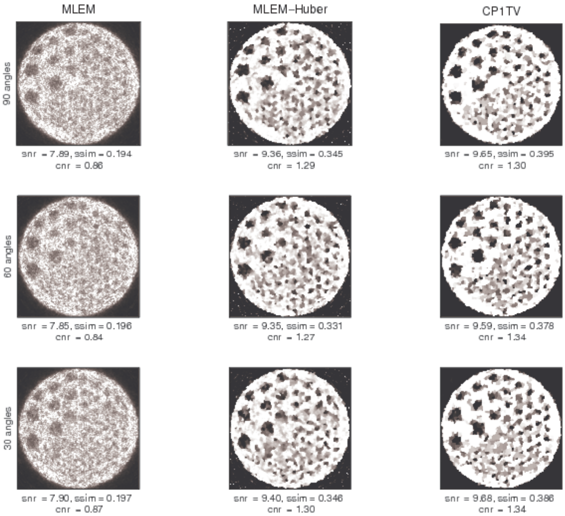

Outline

1 CBCT and PET modeling

2 State of the art

3 Recalls in convex analysis

4 CBCT problem : solvers and results on synthetic data

5 PET problem : solvers and results on synthetic data

6 CBCT problem : results on real data

7 Conclusion

15000 photons per pixel, 60 projections ($\lambda = 15; 25; 40$)

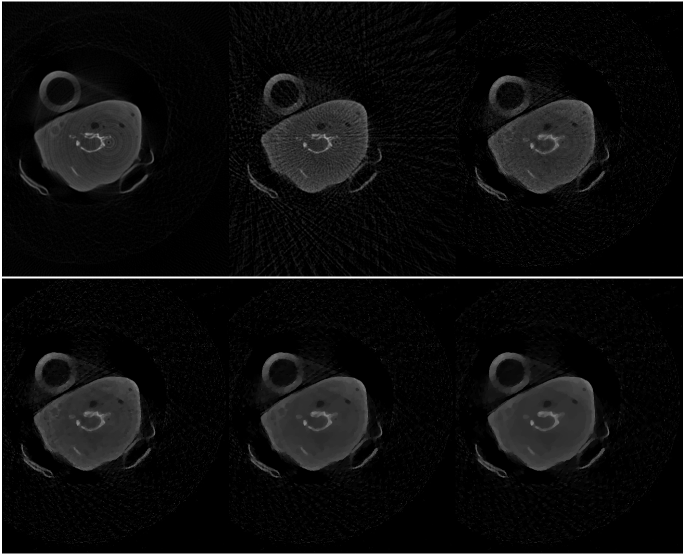

10000 photons per pixel, 60 projections ($\lambda = 15; 25; 40$)

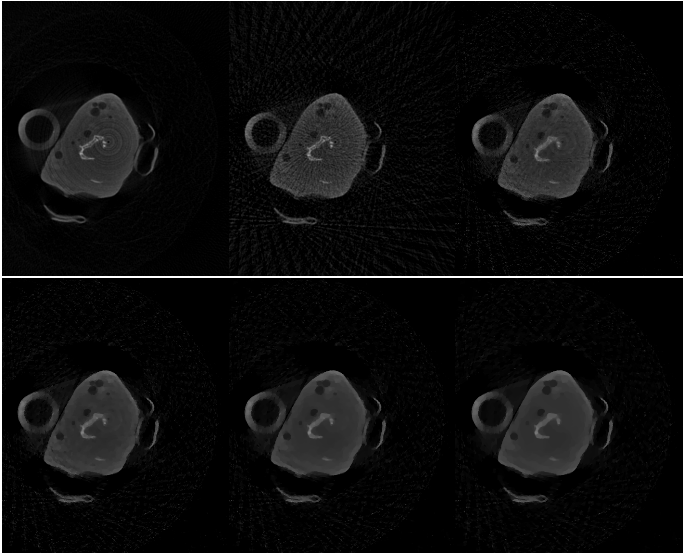

1000 photons per pixel, 60 projections ($\lambda = 15; 25; 40$)

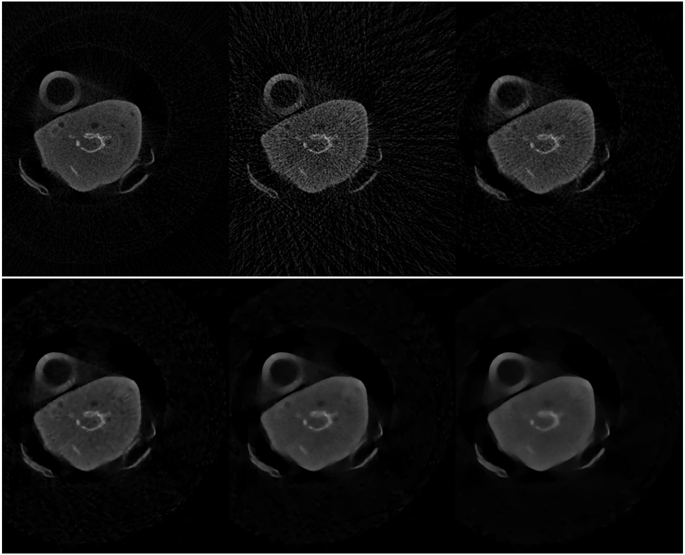

600 photons per pixel, 60 projections ($\lambda = 15; 25; 40$)

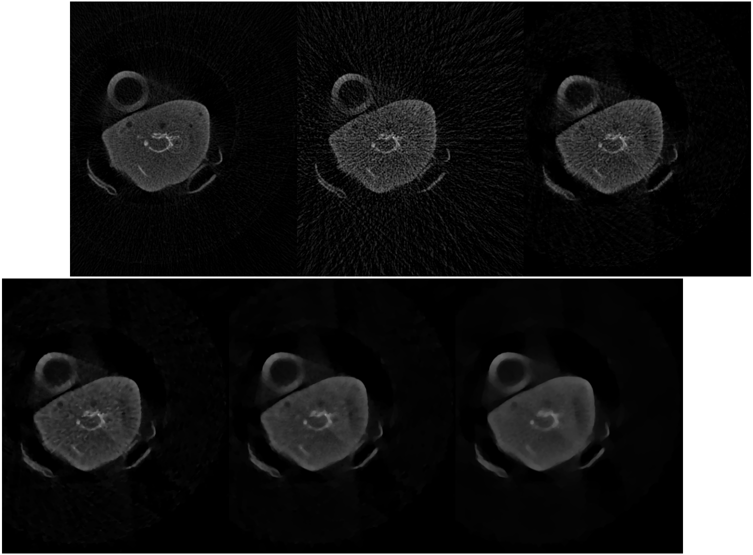

From 2nd to 4th column : nb angles = 90 ; 60 ; 36 ; from top to bottom photon count = 15000 ; 10000 ; 1000 ; 600

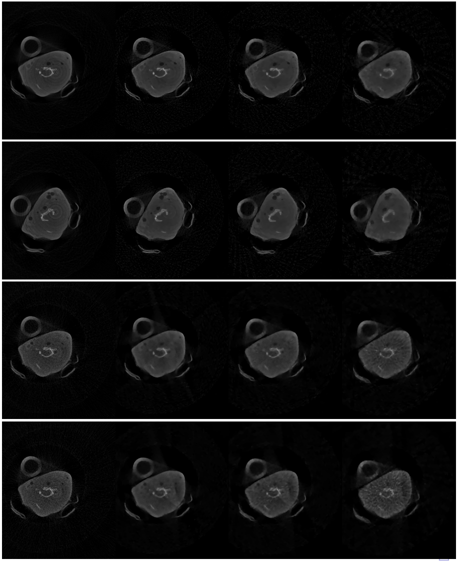

Outline

1. CBCT and PET modeling
2. State of the art
3. Recalls in convex analysis
4. CBCT problem : solvers and results on synthetic data
5. PET problem : solvers and results on synthetic data
6. CBCT problem : results on real data
7. Conclusion

Conclusion

- CT-Scanner based on hybrid pixels.
- Simultaneous PET/CT scanner for bimodality images
- Adapted algorithms : for low photon counts : Poisson noise taken into account, exact physical model.
- For small number of projections : sparse regularizations enhance robustness, and help to have flat by parts images.
- Reconstructions of real acquisitions in the CBCT case confirm the study.
- Real data for the TEP case : wait for the authorization ...
- 3D case : work under progress.

Acceleration in 3D

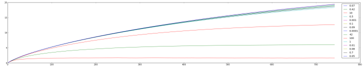

Non accelerated

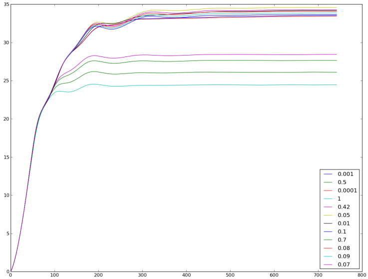

Accelerated